DXA-derived hip shape is associated with hip fracture: a longitudinal study of 38 123 UK Biobank participants

Sophie Scott[1] (iD), Asad Hashmi[1], Raja Ebsim[2], Mijin Jung[1], Fiona R. Saunders[3] (iD),
Jennifer S. Gregory[3], Richard M. Aspden[3] (iD), Claudia Lindner[2] (iD), Timothy Cootes[2],
Nicholas C. Harvey[4,5] (iD), Jonathan H. Tobias[1,6], Benjamin G. Faber[1,6,†*] (iD), Rhona A. Beynon[1,6,†]

[1]Musculoskeletal Research Unit, University of Bristol, Bristol, BS10 5NB, United Kingdom
[2]Division of Informatics, Imaging and Data Sciences, The University of Manchester, Manchester, M13 9PL, United Kingdom
[3]Centre for Arthritis and Musculoskeletal Health, University of Aberdeen, Aberdeen, AB24 2ZD, United Kingdom
[4]Medical Research Council Lifecourse Epidemiology Centre, University of Southampton, Southampton, SO16 6YD, United Kingdom
[5]NIHR Southampton Biomedical Research Centre, University of Southampton and University Hospitals Southampton NHS Foundation Trust, Southampton, SO16 6YD, United Kingdom
[6]Medical Research Council Integrative Epidemiology Unit, University of Bristol, Bristol, BS1 5DS, United Kingdom
*Corresponding author: Benjamin G. Faber, Musculoskeletal Research Unit, Learning and Research Building, Southmead Hospital, Bristol BS10 5FN, United Kingdom (ben.faber@bristol.ac.uk).

Abstract

Despite advancements in fracture prediction tools and osteoporosis management, hip fractures remain a significant consequence of bone fragility, carrying a 22% 1-yr mortality rate. Hip geometric measures (GMs) have been associated with fracture risk; however, their strong correlation hinders the identification of independent influences, leaving their relative predictive value unclear. Statistical shape modeling (SSM) provides a more holistic assessment of hip shape compared to using predetermined GMs. This study aimed to evaluate whether SSM-derived hip shape from DXA scans can predict hip fracture, independently of individual GMs. Previously, we applied SSM to left hip DXA images in UK Biobank—a large prospective cohort with linked hospital records—generating 10 orthogonal hip shape modes (HSMs) that explained 86% of shape variance. Additionally, FN width (FNW), femoral head diameter (FHD), and hip axis length (HAL) were derived from these DXAs. In the current analysis, Cox proportional hazard models, adjusted for age, sex, height, weight, BMD, and GMs (FNW, HAL, and FHD), were used to examine the longitudinal associations between each HSM and first incident hospital diagnosed hip fracture. A Bonferroni adjusted p-value threshold ($p < .004$) was used to account for the 13 exposures. Among the 38 123 participants (mean age 63.7 yr; 52% female; mean follow-up 5 yr), 133 (0.35%) experienced subsequent hip fracture. HSM2, characterized by a narrower FNW, a higher neck shaft angle, and reduced acetabular coverage, showed a strong association with hip fracture risk (HR: 1.32, 95% CI: 1.11-1.58, p: 1.47×10^{-3}), which persisted after full adjustment (1.30, 1.09-1.55, 3.27×10^{-3}). There was no evidence for an association with other HSMs. These findings suggest that DXA-derived hip shape is associated with hip fracture risk independently of BMD and GMs. Incorporating global hip shape into fracture risk assessment tools could enhance prediction accuracy and inform targeted interventions.

Keywords: epidemiology, hip morphology, hip fracture, statistical shape modeling, DXA

Lay Summary

Despite improvements in hip fracture prevention, they remain a major problem, with 22% of people dying within a year of sustaining one. This study looked at medical images from 38 123 individuals in UK Biobank to assess the shape of their hip using computer-aided statistical techniques. The results indicate that a hip shape variation describing a narrower FN and a larger angle linking the neck and the femoral shaft is linked to fracture. This association persisted after accounting for other known hip shape measures related to fracture risk. Therefore, hip shape could help to improve prediction and prevention of hip fractures.

Introduction

The annual number of hip fractures in the UK is projected to rise by 32% over the next 4 yr,[1] highlighting the need for accurate prediction of hip fracture risk. These fractures represent a significant consequence of osteoporosis-related bone fragility and carry a 1-yr mortality rate of 22%.[2] However, not all individuals who sustain a hip fracture meet the diagnostic criteria for osteoporosis,[3] which is primarily based on BMD. Clinical risk assessment tools, such as

FRAX[4]—widely used in over 100 international guidelines—and the UK-specific Qfracture,[5] have been developed to better predict the risk of incident fractures, but still lack optimal sensitivity.[6,7] Consequently, incorporating additional factors not currently considered in existing tools could help improve the accuracy of fracture risk prediction.[8]

Variation in hip shape is increasingly recognized as a contributor to hip fracture,[9,10] having also been linked to osteoarthritis.[11] Hip shape can be assessed through measuring

individual geometric measures (GMs), or by evaluating the overall shape. Common examples of GMs include hip axis length (HAL), neck shaft angle (NSA), FN width (FNW), and femoral head diameter (FHD), which can all be derived from DXA scans, either manually or using software, such as hip structural analysis.[12] Although evidence linking GMs to fracture risk is inconsistent, a recent meta-analysis found that increased HAL, NSA, and FNW are associated with higher fracture risk, with pooled odds ratios (OR) of 1.53, 1.47, and 2.68, respectively.[10] This did not account for factors, such as age and sex. Nonetheless, the International Society of Clinical Densitometry recommends using only HAL for assessing hip fracture risk in females, and advises against using GMs to guide treatment decisions.[12] Moreover, the high correlation between GMs, such as FNW and HAL,[11] as well as the correlation between GMs and body size,[13] complicates the evaluation of their individual contributions to hip fracture risk. In contrast, assessing hip shape as a whole, rather than focusing on individual GMs, may provide a more comprehensive understanding of hip health and fracture risk by accounting for overall morphology and the relationships between different features.[14]

Statistical shape modeling (SSM), a computer-aided technique designed to capture the statistical variability of shapes within a dataset,[15] can be used to provide a more holistic measure of hip shape. Statistical shape modeling uses outline points derived from hip images and employs principal component analysis (PCA) to produce orthogonal modes of shape variation, termed hip shape modes (HSMs),[16] which each capture a different aspect of hip morphology. Although research linking HSMs to hip fracture risk is limited, one study that applied SSM to radiographs found that a HSM characterized by a longer FN, smaller femoral head and a narrower FNW was associated with a higher fracture risk (OR 2.48).[8] Studies comparing SSM-derived measures of hip shape to GMs in the context of hip fractures have been limited to small studies,[9] which have been unable to show that SSM-derived hip fracture risk is independent of GMs. This underscores the need for a comparative analysis to identify the most effective predictors of hip fracture risk. In our recent work using UK Biobank (UKB), we developed a machine-learning algorithm that automatically places outline points on high-resolution hip DXA images,[17] facilitating the generation of hip shape measures in large numbers.

In the present study, we aimed to establish whether SSM-derived hip shape, obtained using our automated point placement method, is associated with hip fracture risk independently of established risk factors and hip GMs, while also analyzing potential sex differences within these associations in the UKB cohort.

Materials and methods
Population

UK Biobank is a prospective cohort study that recruited ~500 000 males and females, aged 40-69 yr, from 22 assessment centers across the UK between 2006 and 2010.[18] Baseline genetic and phenotypic information was obtained through questionnaires, physical measurements, and biological samples. In 2014, UKB launched the Image Enhancement study, which aims to gather imaging data, including hip DXA scans, from 100 000 participants.[19] This
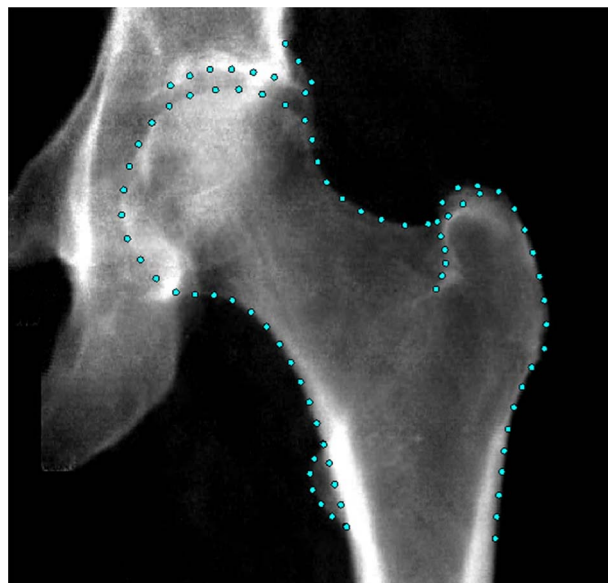

Figure 1. An example hip DXA scan from UKB showing the points placed around the hip joint.

study is overseen by the UKB Ethics Advisory Committee, and ethical approval was given by the National Information Governing Board for Health and Social Care and North-West Multi-centre Research Ethics Committee (11/NW/0382). All participants provided informed consent for their data to be used in the study.

Acquisition of DXA-derived hip shape

Hip DXA images were acquired following a standardized protocol using an iDXA scanner (GE-Lunar), with participants' legs positioned at an internal rotation of 15°-25°.[19] A Random Forest-based machine learning algorithm[20] (BoneFinder, The University of Manchester) had been previously used to automatically place the hip outline points.[17] This algorithm was initially trained on a subset of ~7000 manually marked-up images before being applied to the remaining ~33 000 images. A total of 85 outline points were placed around the femoral head and acetabulum, including the greater and lesser trochanters (Figure 1). The placement of the outline points was manually verified, with only 10% requiring adjustment and an average correction distance of 1.9 mm.[21]

Once outlined, PCA was performed to generate a set of orthogonal HSMs, which collectively explain 100% of the variance.[17] To minimize the burden of multiple testing, this analysis focused on the first ten HSMs (Figure 2), which accounted for 86% of the shape variance within the data set. Subsequent HSMs explained minimal additional shape variance and are unlikely to hold clinical significance. Each individual is given a SD score (mean 0) for each HSM and this describes their propensity toward the positive or negative shapes shown in Figure 2. Additionally, FNW, FHD, and HAL were previously derived from the DXA scans using an openly available custom Python script, as described elsewhere.[11,22]

Ascertainment of hip fracture

Hip fracture data were obtained through linkage to hospital episode statistics (HES), which uses the International Classification of Diseases (ICD) 10th revision codes. Hip fractures were identified based on the following codes: fractured
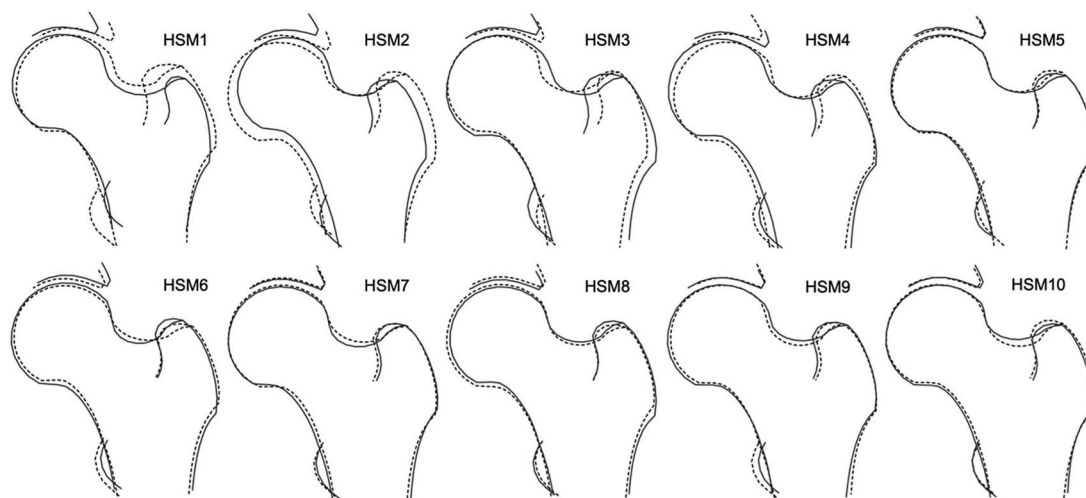
Figure 2. The 10 hip shape modes (HSMs). The solid line shows the shape +2 SD from the mean, and the dotted line shows the shape −2 SDs from the mean.

neck of femur (S72.0), pertrochanteric fracture (S72.1), subtrochanteric fracture (S72.2), stress fracture, not elsewhere classified (pelvic region and thigh) (M84.359), or pathological fracture, not elsewhere classified (pelvic region and thigh) (M84.459) (Table S1). Recording of HES data began on the April 1, 1997. Hip fracture data were downloaded in August 2023, capturing information up until the end of October 2022.

Statistical analysis

Descriptive statistics, including means, SDs, and ranges, were used to summarize population characteristics and the distributions of HSMs and GMs. Histograms were plotted for each HSM to confirm normal distribution. The correlations between each HSM, GM, BMD, and demographic factors (height, weight, and age), were assessed using Pearson correlation coefficient (r). Cox proportional hazard models were used to examine the longitudinal associations between each HSM and hip fracture risk, as well as between each GM (FNW, FHD, and HAL), BMD, ratios of GMs (FNW/FHD and FNW/HAL), and hip fracture risk. The follow-up period concluded at the earliest event, which was either the first incident hip fracture during follow-up, withdrawal, censoring due to death or until the end of the study (October 31, 2022). Individuals who had a hip fracture before attending the imaging assessment, that is, before the DXA scan, were excluded from the analysis. The Cox proportional hazards assumption was tested using the Schoenfeld residuals approach. A Bonferroni adjusted p-value threshold ($p < .004$) was used to account for the 13 exposures tested (10 HSMs and 3 GMs). In a subsample with repeat imaging, concordance correlation coefficient (CCC) and coefficient of variation (CV) were used to assess variation in measures across 2 time points. Coefficient of variation data could not be calculated for HSMs, as they are centered on 0. Kaplan–Meier survival analysis was conducted for HSM2 and each of the GMs. Results are shown as hazard ratios (HR), which represent the relative risk of experiencing a hip fracture over time, with 95% CI and p-values. Hazard ratios are reported per one SD increase in each HSM or GM. Results are presented across 4 models: Model 1 is unadjusted; Model 2 adjusts for demographic characteristics (age, sex, height, and weight); Model 3 additionally adjusts for left

hip total femoral BMD; and Model 4 further adjusts for GMs (FNW, FHD, and HAL). When a GM is the exposure, model 4 adjusts for the other 2 GMs. Both combined-sex and sex-stratified analyses were conducted to account for known disparities in fracture risk[23] and hip shape[24] between males and females. Ethnicity was not included within adjustment models due to 96.7% of the cohort being of white ethnic background, with only 2 fractures observed within participants of other ethnic groups (Table S2). All statistical analyses were performed using STATA version 18 (Stata Corp).

Composite models

To investigate the overall at-risk hip shape for fracture, a composite HSM figure was plotted by combining all HSMs. Briefly, to do this, unadjusted beta coefficients for the associations between HSMs and fracture were first computed. Each beta was then multiplied by 10 to enhance the visualization of shapes, and subsequently multiplied by the HSM-specific SD to account for the contribution of each HSM to the overall shape variance. These adjusted values were combined into a single vector to assess the collective impact of hip shape on hip fracture.

Results
Baseline characteristics

A total of 41 160 left hip DXA images were available prior to the point placement, 40 340 were retained after exclusion for poor image quality, image error, and withdrawal of consent. From these 2217 were excluded due to hip fracture occurring prior to the DXA scan or incomplete covariate data. This resulted in 38 123 left-hip DXA images with outline points delineating the bone contour, which were included in this analysis (Figure S1). The mean age was 63.7 yr, and 52% of participants were female (Table 1). Mean BMD of the left femur was 0.99 g/cm^2, with females having a lower mean BMD (0.93 g/cm^2) compared to males (1.06 g/cm^2). A total of 133 participants (0.35%) had a hip fracture, with a higher prevalence among females (89 cases, 0.45%) compared with males (44 cases, 0.24%). Mean HSM values differed between sexes, with the greatest difference seen in HSM1, HSM3, and HSM9. For the GMs, the combined sex mean for FNW was

Table 1. Descriptive statistics of UK Biobank participants included in this study.

	Combined	Female	Male
	N = 38 123	N = 19 820 (52%)	N = 18 303 (48%)
Exposures	Mean [SD, range]	Mean [SD, range]	Mean [SD, range]
Age (yr)	63.7 [7.6, 44 to 82]	63.0 [7.4, 45 to 82]	64.3 [7.7, 44 to 81]
Height (cm)	170.2 [9.4, 135 to 204]	163.7 [6.4, 135 to 196]	177.2 [6.6, 150 to 204]
Weight (kg)	75.4 [15.1, 34 to 171]	68.2 [12.9, 34 to 169]	83.2 [13.4, 47 to 171]
Left total femoral BMD (g/cm^2)	0.99 [0.16, 0.00 to 1.68]	0.93 [0.14, 0.13 to 1.67]	1.06 [0.14, 0.00 to 1.68]
Hip shape mode 1	0.0 [1.0, −4.6 to 3.9]	0.3 [0.9, −3.8 to 3.9]	−0.3 [1.0, −4.6 to 3.6]
Hip shape mode 2	0.0 [1.0, −4.7 to 4.5]	−0.0 [1.0, −4.7 to 4.2]	0.0 [1.0, −4.5 to 4.5]
Hip shape mode 3	0.0 [1.0, −4.1 to 4.3]	−0.3 [0.9, −4.1 to 4.0]	0.3 [1.0, −3.6 to 4.3]
Hip shape mode 4	0.0 [1.0, −4.4 to 4.0]	−0.1 [1.0, −4.4 to 4.0]	0.1 [1.0, −3.8 to 4.0]
Hip shape mode 5	0.0 [1.0, −4.5 to 3.5]	0.0 [1.1, −4.4 to 3.4]	−0.0 [0.9, −4.5 to 3.5]
Hip shape mode 6	0.0 [1.0, −4.6 to 5.0]	0.2 [1.0, −3.4 to 5.0]	−0.2 [1.0, −4.6 to 3.9]
Hip shape mode 7	0.0 [1.0, −4.9 to 5.0]	0.1 [1.0, −4.9 to 4.7]	−0.1 [1.0, −4.6 to 5.0]
Hip shape mode 8	0.0 [1.0, −4.4 to 4.5]	−0.1 [1.0, −4.4 to 4.0]	0.1 [1.0, −4.0 to 4.5]
Hip shape mode 9	0.0 [1.0, −4.1 to 5.0]	−0.3 [0.9, −4.1 to 4.5]	0.3 [1.0, −3.7 to 5.0]
Hip shape mode 10	0.0 [1.0, −4.1 to 3.8]	0.0 [1.0, −4.1 to 3.8]	−0.0 [1.0, −4.1 to 3.8]
Narrowest neck width (mm)	31.6 [3.5, 21.4 to 45.8]	29.0 [2.0, 21.4 to 37.8]	34.5 [2.4, 22.9 to 45.8]
Diameter of femoral head (mm)	45.9 [3.8, 33.4 to 64.4]	43.0 [2.3, 33.4 to 53.7]	49.0 [2.6, 34.7 to 64.4]
Hip axis length (mm)	96.7 [8.0, 68.1 to 127.1]	90.8 [4.8, 68.1 to 115.5]	103.1 [5.5, 76.9 to 127.1]
	Number fractured [%]	Number fractured [%]	Number fractured [%]
Hospital diagnosed fracture	133 [0.35]	89 [0.45]	44 [0.24]
	Mean [SD, range]	Mean [SD, range]	Mean [SD, range]
Time to end of study (yr)	5.0 [1.5, 0.2 to 8.5]	5.0 [1.5, 0.1 to 8.5]	5.0 [1.5, 0.2 to 8.5]

Population characteristics of the UK Biobank participants included in this study with complete data for all covariates.

31.6 mm, FHD was 45.9 mm, and HAL was 96.7 mm. Males had a greater mean FNW, FHD, and HAL than females. The mean follow-up period was 5.0 yr (median = 4.6 yr, IQR = 3.8-6.2 yr). The incidence rate for hip fractures were 0.69 fractures per 1000 person years.

Geometric measures, their inter-relationships, and reliability

Femoral head diameter, FNW, and HAL were all highly correlated with each other (*r*: 0.81-0.89) and with height (*r*: 0.75-0.81) (Figure S2). Weight was moderately correlated with FHD, FNW, HAL, height, and BMD (*r*: 0.52-0.57). The HSMs were orthogonal by design. Similarly, no correlation was observed between the HSMs and the other covariates. In a subsample of 354 individuals with imaging on average 2.3 yr later, good agreement was seen between GM, BMD, and HSM measures (CCC: 0.70-0.99) except HSM5 (CCC: 0.51) (Table S3).

Geometric measures and their association to hip fracture

Femoral neck width

In the unadjusted analysis of all participants (Figure 3, Table S4), FNW was not associated with hip fracture (Model 1: 1.15, 0.97-1.36, 0.11). However, a strong association was seen between a wider FNW and hip fracture following adjustment for demographic characteristics and BMD (Model 3: 1.77, 1.30-2.43, 3.26×10^{-4}). In sex-stratified analysis (Table S4), a wider FNW showed a strong association with hip fracture in both sexes, both in the unadjusted model and following adjustment for demographic characteristics. In males, the strongest association was observed in the unadjusted model (Model 1: 2.17, 1.44-3.25, 1.99×10^{-4}). The association weakened with adjustment for BMD (Model 3: 1.75, 1.08-2.82, 0.02). A similar trend was noted in females,

with the strongest association being in the unadjusted model (Model 1: 2.88, 2.05-4.06, 1.40×10^{-9}). Further adjustment for BMD resulted in attenuation (Model 3: 1.70, 1.11-2.59, 0.01). The effect sizes were greater in females compared to males in models 1 and 2, with a similar effect size seen in both sexes in model 3.

Femoral head diameter

In the unadjusted analysis of all participants, there was little evidence for an observed association between FHD and hip fracture (Model 1: 1.12, 0.95-1.53, 0.17) (Figure 3, Table S4). However, a strong positive association was seen when adjusting for BMD (Model 3: 1.89, 1.39-2.57, 4.48×10^{-5}). In the unadjusted sex-stratified analysis, a larger FHD demonstrated a greater effect size in females compared with males (Model 1—females: 2.43, 1.73-4.30, 2.60×10^{-7}; males: 2.30, 1.54-3.44, 4.50×10^{-5}). When adjusting for BMD, a larger effect size was seen in males compared with females (Model 3—males: 2.01, 1.28-3.14, 2.26×10^{-3}; females: 1.70, 1.11-2.60, 0.01).

Hip axis length

Similar to FNW and FHD, HAL did not show an association with hip fracture in unadjusted analysis of all participants (Model 1: 1.08, 0.91-1.28, 0.39) (Figure 3, Table S4). However, an increased HAL was associated with hip fracture after adjusting for BMD (Model 3: 1.61, 1.18-2.21, 3.08×10^{-3}). When compared with FNW and FHD, HAL exhibited the smallest effect size across all models. A strong positive association was seen only in the unadjusted sex-stratified analysis (Model 1—males: 2.07, 1.37-3.11, 4.84×10^{-4}; females: 2.05, 1.48-2.85, 1.58×10^{-5}) (Table S4), with the associations seen diminishing after further adjustment for BMD (Model 3—males: 1.84, 1.11-3.04, 0.02; females: 1.40, 0.92-2.13, 0.11).
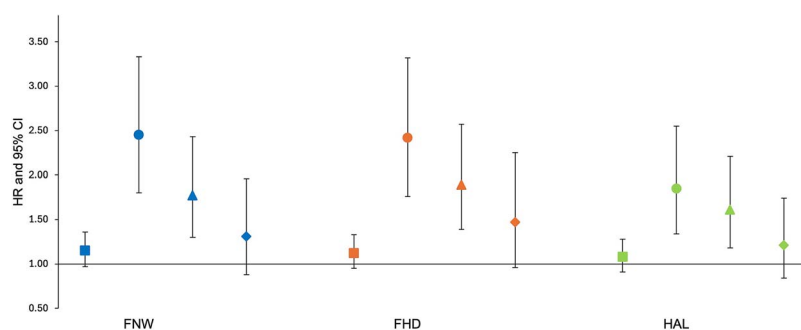
Figure 3. Cox proportional hazard results for the association between each geometric measure (GM) and hip fracture in combined sex analysis. Hazard ratios (HR) with 95% CIs are plotted. Hazard ratios are reported per 1 SD increase in each hip shape mode. Square = unadjusted (model 1); circle = adjusted for age, sex, height, and weight (model 2); triangle = adjusted for model 2 plus BMD (model 3); diamond = fully adjusted for model 3 plus the other 2 GMs (model 4). Abbreviations: FHD, femoral head diameter; FNW, femoral neck width; HAL, hip axis length.

Mutual adjustment and ratios of geometric measures

When each GM was mutually adjusted for the other 2 GMs, along with demographic characteristics and BMD, there was less evidence for an association with hip fracture in both combined and sex-stratified analysis. All results fell below the statistical significance threshold for multiple testing (Figure 3, Table S4). Ratios of GMs were analyzed to account for the high correlations between individual measures. In combined-sex analysis, the FNW/HAL ratio was significantly associated with hip fracture after adjusting for demographic characteristics (1.33, $1.11\text{-}1.59$, 1.92×10^{-3}). In sex-stratified analyses, none of the ratios were statistically significant in males. In females, both ratios were associated with hip fracture in the unadjusted model, but only the FNW/HAL ratio remained significant after adjustment for demographic characteristics (1.41, $1.12\text{-}1.77$, 3.27×10^{-3}) (Table S4).

Association between HSMs and hip fracture

Each HSM was initially assessed for its association with hip fracture. In the unadjusted combined-sex analysis, there was evidence of a strong positive association between HSM2 (Figure 4) and hip fracture (Model 1—HR: 1.32, 95% CI: $1.11\text{-}1.56$, $p = 1.47 \times 10^{-3}$) (Figure 5, Table 2). This association persisted upon adjustment for demographic characteristics and BMD (Model 3: 1.31, $1.11\text{-}1.55$, 1.51×10^{-3}). Put simply, fracture risk is increased by approximately 30% in individuals with HSM2 values exceeding 1 SD, representing approximately 15.4% of the population. HSM2 captures features of a narrower FNW, a higher NSA, and reduced acetabular coverage (Figure 2). No other HSMs were found to be associated with hip fracture in combined-sex analysis.

In female sex-stratified analysis (Table S5), HSM2 showed a positive association with hip fracture when adjusted for demographic characteristics (Model 2: 1.37, $1.11\text{-}1.68$, 2.79×10^{-3}). Apart from this, sex-stratified analyses failed to show statistical evidence for an association with hip fracture potentially, because they were underpowered.

To evaluate the association between each HSM and hip fracture risk, independent of the hip shape components captured by GMs, each HSM was further adjusted for all 3 GMs (FNW, FHD, and HAL) (Figure 5, Table 2). Analysis of all participants showed that the associations seen in Models 1, 2, and 3 were maintained after adjusting for demographic characteristics, BMD, and GMs. HSM2 emerged as the only HSM to show strong evidence of an association with hip

fracture in this model (Model 4: 1.30, $1.09\text{-}1.55$, 3.27×10^{-3}). In sex-stratified analysis (Table S5), none of the associations met the Bonferroni-adjusted p-value threshold. However, HSM2 showed weak evidence of an association with hip fracture when fully adjusted in both females and males (Model 4—females: 1.27, $1.03\text{-}1.57$, 0.02; males: 1.34, $0.96\text{-}1.84$, 0.06). HSM9, characterized by larger lesser trochanters and a narrower FN, continued to show weak evidence of a negative association with hip fracture risk in males after full adjustment (Model 4: 0.66, $0.48\text{-}0.89$, 0.01). No other HSM was associated with hip fracture when fully adjusted in either sex. Kaplan–Meier survival analyses stratified for HSM2 and each GM are included in Figure S3.

Association between BMD and hip fracture risk

For comparison, higher total left femoral BMD was strongly associated with a reduced risk of hip fracture in combined-sex (Model 2: 0.36, $0.30\text{-}0.43$, 2.86×10^{-28}) and sex-stratified analysis (Model 2—females: 0.34, $0.27\text{-}0.43$, 2.71×10^{-20}; males: 0.38, $0.28\text{-}0.53$, 4.74×10^{-9}) (Table S6).

Composite model

The composite model (Figure 6) showed that the overall at-risk shape, which is represented by the solid line, included a narrower FNW, reduced acetabular coverage, smaller greater trochanters, and a smaller FHD. This closely reflects HSM2, which shares these shape characteristics.

Discussion

This large, longitudinal cohort study explored the relationship between DXA-derived HSMs and GMs with hip fracture risk. The findings indicate that HSM2, characterized by a narrower FNW, higher NSA, smaller femoral head, and reduced acetabular coverage, was positively associated with hip fracture risk, even after adjusting for age, sex, height, weight and BMD. While GMs (FNW, FHD, and HAL) also showed associations with hip fracture when adjusted for the same covariates, these relationships attenuated upon mutual adjustment, confirming their inter-relatedness. In contrast, HSM2 retained its association with hip fracture after accounting for GMs, suggesting that HSM2 captures additional information beyond these 3 measures of hip geometry.

Currently, there are few comparative studies in the literature that have investigated the association between SSM-derived hip shape and hip fractures. Furthermore, these studies have
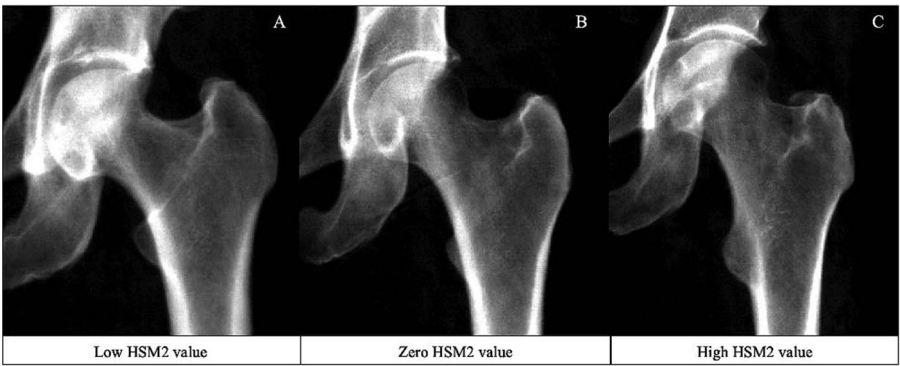
Figure 4. DXA images illustrating high, zero, and low HSM2 scores in women aged 60 yr. The high HSM2 value represents a value >2 SDs above the mean; the average image corresponds to a score of 0; and the low HSM2 value represents a value <2 SDs below the mean. (A) The low HSM2 image shows an individual with a HSM2 score of −3.03. (B) The zero HSM2 image shows an individual with a HSM2 score of 0.01. (C) The high HSM2 image shows an individual with a HSM2 score of 2.56. Abbreviation: HSM, hip shape mode.
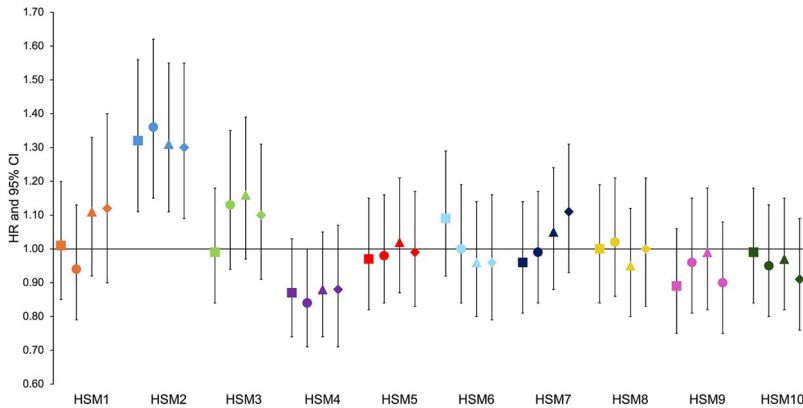

Figure 5. Cox proportional hazard results for the association between each hip shape mode (HSM) and hip fracture in combined sex analysis. Hazard ratios (HRs) with 95% CI are plotted. Hazard ratios are reported per 1 SD increase in each hip shape mode. Square = unadjusted (model 1); circle = adjusted for age, sex, height, and weight (model 2); triangle = adjusted for model 2 plus BMD (model 3); diamond = fully adjusted for model 3 plus the 3 GMs (model 4). Fracture risk is increased by approximately 30% in those who HSM2 value exceeds 1 SD, representing approximately 15.4% of the population.

Table 2. Cox proportional hazard results for the association between each hip shape mode and hip fracture in combined sex analysis.

Exposure	Model 1		Model 2		Model 3		Model 4	
	HR [95% CI]	*p*-value	HR [95% CI]	*p*-value	HR [95% CI]	*p*-value	HR [95% CI]	*p*-value
Hip shape mode 1	1.01 [0.85-1.20]	.91	0.94 [0.79-1.13]	.52	1.11 [0.92-1.33]	.27	1.12 [0.90-1.40]	.33
Hip shape mode 2	1.32 [1.11-1.56]	1.47×10^{-3}	1.36 [1.15-1.62]	3.3×10^{-4}	1.31 [1.11-1.55]	1.51×10^{-3}	1.30 [1.09-1.55]	3.27×10^{-3}
Hip shape mode 3	0.99 [0.84-1.18]	.94	1.13 [0.94-1.35]	.19	1.16 [0.97-1.39]	.10	1.10 [0.91-1.31]	.33
Hip shape mode 4	0.87 [0.74-1.03]	.11	0.84 [0.71-1.00]	.05	0.88 [0.74-1.05]	.17	0.88 [0.71-1.07]	.20
Hip shape mode 5	0.97 [0.82-1.15]	.74	0.98 [0.84-1.16]	.86	1.02 [0.87-1.21]	.79	0.99 [0.83-1.17]	.89
Hip shape mode 6	1.09 [0.92-1.29]	.31	1.00 [0.84-1.19]	1.00	0.96 [0.80-1.14]	.63	0.96 [0.79-1.16]	.68
Hip shape mode 7	0.96 [0.81-1.14]	.66	0.99 [0.84-1.17]	.93	1.05 [0.88-1.24]	.60	1.11 [0.93-1.31]	.25
Hip shape mode 8	1.00 [0.84-1.19]	.99	1.02 [0.86-1.21]	.82	0.95 [0.80-1.12]	.53	1.00 [0.83-1.21]	.98
Hip shape mode 9	0.89 [0.75-1.06]	.19	0.96 [0.81-1.15]	.68	0.99 [0.82-1.18]	.87	0.90 [0.75-1.08]	.26
Hip shape mode 10	0.99 [0.84-1.18]	.93	0.95 [0.80-1.13]	.59	0.97 [0.82-1.15]	.74	0.91 [0.76-1.09]	.30

Hazard ratios (HR) with 95% CI and *p*-values are shown for each hip shape mode and their association to hip fracture. Hazard ratios are reported per 1 SD increase in each hip shape mode. Model 1 = unadjusted; model 2 = adjusted for age, sex, height, and weight; model 3 = adjusted for model 2 plus BMD; model 4 = adjusted for model 3 plus the geometric measures.

derived their SSM from different populations, meaning it is not possible to draw direct comparisons between specific HSMs. For instance, Gregory et al. applied a SSM consisting of 29 points outlining the femoral head and neck to standard radiographs in a small group of females (26 cases, 24 controls).[9] They found that SSM-derived hip shape predicted fracture risk after adjusting for height and weight. Specifically, a HSM with a longer, narrower FN and a higher NSA was

more likely to fracture, reflecting the at-risk shape identified in this study. However, their sample size was considerably smaller than that of our current study and the outline points on the radiographs used to perform SSM did not include the lesser trochanter. Baker-LePain et al. used a similar approach in a nested case-control study involving Caucasian females (168 cases, 231 controls).[8] They employed a larger number of outline points (*n* = 60) than Gregory et al. (*n* = 29), and
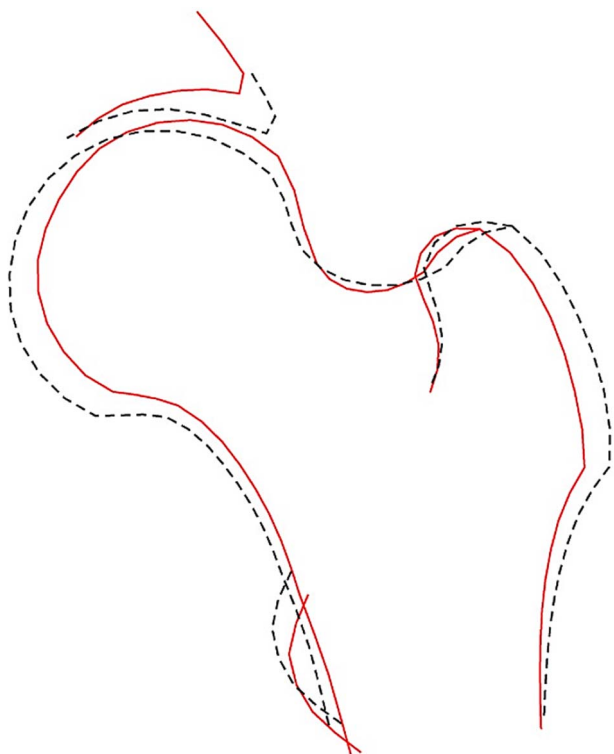
Figure 6. Composite image of the 10 hip shape modes. The solid line shows the shape at risk of fracture, the dotted line shows the mean shape.

their model included the lesser trochanter. They found that hips exhibiting extreme values of HSM4, characterized by a narrower FNW, increased FN length, and a smaller femoral head, were associated with hip fracture. These features closely resemble the at-risk hip shape identified in this study (narrower FNW and smaller femoral head). Although Baker-LePain et al. adjusted for age, body mass index, and FN BMD, they, like Gregory et al., only included females within their analyses, leaving it unclear whether the observed relationships are sex-specific. Goodyear et al. performed SSM using 72 outline points on DXA scans of females aged over 75 yr (182 subjects, 364 controls).[25] The authors identified a hip shape associated with fracture that also closely resembles the findings of our study, including a narrower FNW, greater NSA, reduced acetabular coverage, and smaller greater trochanters. This study offers the closest comparison to the present analysis, as it was performed on DXA scans and used similar outline points, including the acetabulum and lesser trochanter. However, the sample size was smaller, and analysis focused on females only. This limitation is significant, because HSMs are known to be influenced by sex,[26] and our study found notable differences in HSMs between the sexes. Furthermore, none of the studies adjusted for GMs.

Although the at-risk hip shape (HSM2) identified in this study was characterized by a narrower FNW, the analysis of GMs and hip fracture revealed that a wider FNW was associated with hip fracture (Figure 3, Table S4). Our findings are consistent with a recent meta-analysis, as we also observed that a greater FNW and HAL were associated with an increased risk of hip fracture.[10] This finding has been reported in other observational studies,[27–29] including a recent genetic analysis[30] that found that individuals with a genetic predisposition to a greater FNW were at higher risk of fracture. The seemingly contradictory findings between HSM and GMs regarding FNW and fracture risk may be attributable to several factors. Geometric measures objectively quantify individual aspects of hip morphology, meaning that bone size can impact the magnitude of the measurement. For example, larger individuals are likely to have a bigger femur across all dimensions; thus, a taller and heavier person would be expected to have a larger FNW and HAL. Moreover, FNW is highly correlated with height and moderately correlated with weight (Figure S2), a relationship that has been consistently reported in other studies,[11,31] highlighting the significant influence of demographic characteristics, such as height and weight, on FNW. In contrast, SSM employs Procrustes analysis to align and scale hip outlines based on shape, effectively capturing bone morphology while excluding the influence of individual size. This ability to isolate shape from size is important, because HSM2 remained associated with hip fracture risk, independent of FNW, FHD, and HAL. This suggests that these individual measures are not independently driving hip fracture risk. Instead, the interactions and combined influence of these factors, effectively captured by SSM, likely contribute to fracture risk. Ratios of GMs have been suggested as an alternative, aiming to reduce the influence of correlation by standardizing measures against one GM.[13] However, SSM still outperformed ratio values in a previous small study.[9] In this study, ratios of GMs were not more strongly associated with hip fracture than individual GMs, suggesting that these ratios do not provide additional predictive value beyond individual measures or SSM.

The addition of BMD attenuated the association between HSM2 and subsequent hip fracture risk. This is likely due to BMD being a composite of BMC and bone area,[32] the latter of which overlaps with bone shape and geometry. Although BMD is a strongly validated predictor of hip fracture[4] and was more predictive in this study population, our results suggest that SSM derived hip shape could provide complementary information. Further work is needed to determine whether incorporating SSM-derived hip shape into fracture risk models, such as FRAX, would provide significant improvement to justify its inclusion.

Previous research has explored sex differences in hip shape[24,26,33,34]; few studies have examined these differences within the context of hip fractures. HSM2 showed similar effect sizes between the sexes, but a notable difference was seen with HSM9 (Table S5). Studies of individual hip shape measures have shown that females tend to have a smaller FHD, narrower FNW, and shorter FN length compared to males,[34] which likely reflects that females are typically smaller than males. Similarly, Frysz et al. found sex differences in HSMs, with females exhibiting a narrower FNW and smaller lesser trochanter compared with males.[26] This finding is noteworthy, particularly given the weak evidence of a negative association with hip fracture seen with HSM9 in males (Table S5). HSM9 was characterized by a larger lesser trochanter but a narrower FN, suggesting that a larger lesser trochanter, a feature more common in male hip shapes, could offer some protective effect against hip fracture. Since the lesser trochanter serves as the insertion point for hip flexor muscles,[35] its size could be indicative of muscle mass. Given that sarcopenia (loss of muscle mass and function)[36,37] is a known risk factor for hip fracture,[38–41] a larger lesser trochanter may represent a proxy for muscle strength and function, potentially reducing fracture risk in

males. Additionally, innate female hip shape characteristics may predispose females to a higher fracture risk, as they often exhibit features linked to fractures, such as a narrower FNW. Interestingly, although HSM9 included a narrower FNW, similar to the fracture-prone HSM2, this reinforces the idea that fracture risk is influenced by multiple interacting shape constituents rather than any single measurement.

This study has several key strengths. Its large sample size and population-based design greatly enhances the representativeness of the findings, thereby improving the reliability of effect estimates. By using a CCC and CV, we have shown that our measures are reliable over a two year time frame, and that HSM2 was the most reliable HSM (CCC: 0.93). The study also simultaneously examined the relationship between SSM-derived hip shape and GMs with hip fracture, allowing for a direct comparison of these 2 methods and an evaluation of their independent associations with fracture risk. One of the limitations of SSM is that each study uses a different population to derive their HSMs, thus you cannot compare across models. This UKB model could provide a reference for other populations. Both the SSM-derived hip shape and the GMs were semi-automatically derived from DXA scans, requiring minimal manual point correction. Given the widespread use of DXA scans in clinical practice for assessing osteoporosis, this approach makes accommodating SSM-derived hip shape measures through tools like FRAX a feasible option. Previous studies have shown that SSM can be applied to the DXAs obtained from different types of scanner, with comparable results.[42] Although further work is justified to confirm this before clinical adoption of these methods. Additionally, the inclusion of both combined and sex-stratified analyses represents a significant strength of this study. While many studies primarily examine post-menopausal females, this study also included male participants, providing valuable insights into male hip shape and its role in fracture risk.

There are limitations to this study. As an observational study, it cannot establish causality. Further research to understand the factors driving the association between HSM2 and hip fracture risk is needed, although a recent study using genetic data found evidence of a causal association between HSM2 and hip fracture in the same population.[43] Neck shaft angle could not be derived from the DXA scans due to the limited view of the femoral shaft. Given that prior studies have linked higher NSA to hip fracture, and HSM2 represents a higher NSA, we were unable to determine if the association between HSM2 and hip fracture was independent of NSA.[10,31] The predominantly Caucasian study population may limit the generalizability of the findings. Notably, differences in hip shape have been reported between UKB participants and the exclusively Chinese Shanghai Changfeng cohort.[44] The mean age of participants (63.7 yr) may have reduced the study's power, as hip fractures predominantly occur in older individuals.[45] However, as participants continue to be followed-up and additional DXA images from UKB become available, analysis can be repeated with more hip fracture cases, potentially strengthening findings. It should be acknowledged that while hip structural analysis is readily available, implementing SSM in clinical practice would require additional resources and technology. Since the analysis focused only on left hip DXA scans, and the side of the body the hip fracture occurred on is unknown, it is plausible that effect estimates could be biased toward the null. As a result, the true effect of hip shape on fracture risk may be underestimated or not fully captured in the analysis. Furthermore, using 2D DXA scans to assess the shape of a 3D structure may result in the loss of spatial detail; however, SSM can help mitigate these limitations by using proportional rather than absolute values of hip shape as described by GMs.[9]

In conclusion, this study examined SSM-derived hip shape using high-resolution DXA scans from a large cohort of UKB participants, demonstrating risk of incident hip fracture is higher with a narrower FN, a higher FN angle and reduced acetabular coverage. Importantly, these associations were independent of a wide range of covariates including established measures of femoral geometry. Given that DXA scans are already routinely used to assess osteoporosis risk, further work is justified to investigate whether SSM-derived measures of hip shape could be accommodated into existing fracture risk tools, such as FRAX, to improve prediction. This approach could facilitate targeted preventative treatments for individuals with hip shapes resembling HSM2, thereby reducing the risk of hip fractures and alleviating the resultant morbidity and mortality.

Acknowledgments

Author contributions

Sophie Scott (Data curation, Formal analysis, Software, Visualization, Writing—original draft, Writing—review & editing), Asad Hashmi (Data curation, Formal analysis, Software, Writing—review & editing), Raja Ebsim (Conceptualization, Funding acquisition, Methodology, Writing—review & editing), Mijin Jung (Data curation, Formal analysis, Software, Writing—review & editing), Fiona R. Saunders (Conceptualization, Funding acquisition, Methodology, Writing—review & editing), Jennifer S. Gregory (Conceptualization, Funding acquisition, Methodology, Writing—review & editing), Richard M. Aspden (Conceptualization, Funding acquisition, Methodology, Writing—review & editing), Claudia Lindner (Conceptualization, Funding acquisition, Methodology, Writing—review & editing), Timothy Cootes (Conceptualization, Funding acquisition, Methodology, Writing—review & editing), Nicholas C. Harvey (Conceptualization, Funding acquisition, Methodology, Writing—review & editing), Jonathan H. Tobias (Conceptualization, Funding acquisition, Methodology, Supervision, Validation, Writing—review & editing), Benjamin G. Faber (Conceptualization, Data curation, Formal analysis, Funding acquisition, Investigation, Methodology, Project administration, Resources, Software, Supervision, Validation, Visualization, Writing—original draft, Writing—review & editing), and Rhona A. Beynon (Conceptualization, Data curation, Formal analysis, Funding acquisition, Investigation, Methodology, Project administration, Resources, Software, Supervision, Validation, Visualization, Writing—original draft, Writing—review & editing)

Benjamin G. Faber and Rhona A. Beynon are joint senior authors.

Supplementary material

Supplementary material is available at *Journal of Bone and Mineral Research* online.

Conflicts of interest

The authors have no conflicts of interest to disclose.

Data availability

All data variables are available from UK Biobank. The BoneFinder search model and the SSM can be requested via the BoneFinder website for independent validation: https://bone-finder.com/.

Ethics statement

This study is overseen by the UKB Ethics Advisory Committee, and ethical approval was given by the National Information Governing Board for Health and Social Care and North-West Multi-centre Research Ethics Committee (11/NW/0382). All participants provided informed consent for their data to be used in the study.

References

1. Harris E, Clement N, MacLullich A, Farrow L. The impact of an ageing population on future increases in hip fracture burden. *Bone Joint J*. 2024;106-b(1):62-68. https://doi.org/10.1302/0301-620x.106b1.bjj-2023-0740.r1
2. Downey C, Kelly M, Quinlan JF. Changing trends in the mortality rate at 1-year post hip fracture - a systematic review. *World J Orthop*. 2019;10(3):166-175. https://doi.org/10.5312/wjo.v10.i3.166
3. Schuit SCE, van der Klift M, Weel AEAM, et al. Fracture incidence and association with bone mineral density in elderly men and women: the Rotterdam study. *Bone*. 2004;34(1):195-202. https://doi.org/10.1016/j.bone.2003.10.001
4. Kanis JA, Harvey NC, Cooper C, Johansson H, Odén A, McCloskey EV. A systematic review of intervention thresholds based on FRAX : a report prepared for the National Osteoporosis Guideline Group and the International Osteoporosis Foundation. *Arch Osteoporos*. 2016;11(1):25. https://doi.org/10.1007/s11657-016-0278-z
5. Hippisley-Cox J, Coupland C, Brindle P. The performance of seven QPrediction risk scores in an independent external sample of patients from general practice: a validation study. *BMJ Open*. 2014;4(8):e005809. https://doi.org/10.1136/bmjopen-2014-005809
6. Gregson CL. CFracture, an alternative to QFracture that accounts for mortality to better predict fragility fracture risk. *Lancet Healthy Longev*. 2023;4(1):e6-e7. https://doi.org/10.1016/S2666-7568(22)00293-8
7. Kanis JA, Compston J, Cooper C, et al. SIGN Guidelines for Scotland: BMD versus FRAX versus QFracture. *Calcif Tissue Int*. 2016;98(5):417-425. https://doi.org/10.1007/s00223-015-0092-4
8. Baker-LePain JC, Luker KR, Lynch JA, Parimi N, Nevitt MC, Lane NE. Active shape modeling of the hip in the prediction of incident hip fracture. *J Bone Miner Res*. 2011;26(3):468-474. https://doi.org/10.1002/jbmr.254
9. Gregory JS, Testi D, Stewart A, Undrill PE, Reid DM, Aspden RM. A method for assessment of the shape of the proximal femur and its relationship to osteoporotic hip fracture. *Osteoporos Int*. 2004;15(1):5-11. https://doi.org/10.1007/s00198-003-1451-y
10. Fajar JK, Taufan T, Syarif M, Azharuddin A. Hip geometry and femoral neck fractures: a meta-analysis. *J Orthop Translat*. 2018;13:1-6. https://doi.org/10.1016/j.jot.2017.12.002
11. Heppenstall SV, Ebsim R, Saunders FR, et al. Hip geometric parameters are associated with radiographic and clinical hip osteoarthritis: findings from a cross-sectional study in UK Biobank. *Osteoarthr Cartil*. 2023;31(12):1627-1635. https://doi.org/10.1016/j.joca.2023.09.001
12. Broy SB, Cauley JA, Lewiecki ME, Schousboe JT, Shepherd JA, Leslie WD. Fracture risk prediction by non-BMD DXA measures: the 2015 ISCD official positions part 1: hip geometry. *J Clin Densitom*. 2015;18(3):287-308. https://doi.org/10.1016/j.jocd.2015.06.005
13. Gregory JS, Aspden RM. Femoral geometry as a risk factor for osteoporotic hip fracture in men and women. *Med Eng Phys*. 2008;30(10):1275-1286. https://doi.org/10.1016/j.medengphy.2008.09.002
14. Bredbenner TL, Mason RL, Havill LM, Orwoll ES, Nicolella DP, Study ftOFiM. Fracture risk predictions based on statistical shape and density modeling of the proximal femur. *J Bone Miner Res*. 2014;29(9):2090-2100. https://doi.org/10.1002/jbmr.2241
15. Ambellan F, Lamecker H, von Tycowicz C, Zachow S. Statistical shape models: understanding and mastering variation in anatomy. *Adv Exp Med Biol*. 2019;1156:67-84. https://doi.org/10.1007/978-3-030-19385-0_5
16. Johnson LG, Bortolussi-Courval S, Chehil A, et al. Application of statistical shape modeling to the human hip joint: a scoping review. *JBI Evid Synth*. 2023;21(3):533-583. https://doi.org/10.11124/jbies-22-00175
17. Frysz M, Faber BG, Ebsim R, et al. Machine learning-derived acetabular dysplasia and cam morphology are features of severe hip osteoarthritis: findings from UK Biobank. *J Bone Miner Res*. 2022;37(9):1720-1732. https://doi.org/10.1002/jbmr.4649
18. Bycroft C, Freeman C, Petkova D, et al. The UK Biobank resource with deep phenotyping and genomic data. *Nature*. 2018;562(7726):203-209. https://doi.org/10.1038/s41586-018-0579-z
19. Littlejohns TJ, Holliday J, Gibson LM, et al. The UK Biobank imaging enhancement of 100,000 participants: rationale, data collection, management and future directions. *Nat Commun*. 2020;11(1):2624. https://doi.org/10.1038/s41467-020-15948-9
20. Lindner C, Thiagarajah S, Wilkinson JM, Wallis GA, Cootes TF. Development of a fully automatic shape model matching (FASMM) system to derive statistical shape models from radiographs: application to the accurate capture and global representation of proximal femur shape. *Osteoarthr Cartil*. 2013;21(10):1537-1544. https://doi.org/10.1016/j.joca.2013.08.008
21. Faber BG, Ebsim R, Saunders FR, et al. A novel semi-automated classifier of hip osteoarthritis on DXA images shows expected relationships with clinical outcomes in UK Biobank. *Rheumatology (Oxford)*. 2021;61(9):3586-3595. https://doi.org/10.1093/rheumatology/keab927
22. Faber B. Geometric Parameters Python 3.0 Code. 2022. https://zenodo.org/badge/latestdoi/518486087.
23. Holroyd C, Cooper C, Dennison E. Epidemiology of osteoporosis. *Best Pract Res Clin Endocrinol Metab*. 2008;22(5):671-685. https://doi.org/10.1016/j.beem.2008.06.001
24. Wang SC, Brede C, Lange D, et al. Gender differences in hip anatomy: possible implications for injury tolerance in frontal collisions. *Annu Proc Assoc Adv Automot Med*. 2004;48:287-301.
25. Goodyear SR, Barr RJ, McCloskey E, et al. Can we improve the prediction of hip fracture by assessing bone structure using shape and appearance modelling? *Bone*. 2013;53(1):188-193. https://doi.org/10.1016/j.bone.2012.11.042
26. Frysz M, Gregory J, Aspden RM, Paternoster L, Tobias JH. Sex differences in proximal femur shape: findings from a population-based study in adolescents. *Sci Rep*. 2020;10(1):4612. https://doi.org/10.1038/s41598-020-61653-4

27. Fajar JK, Rusydi R, Rahman S, Alam AIN, Azharuddin A. Hip geometry to predict femoral neck fracture: only neck width has significant association. *Apollo Med*. 2016;13(4):213-219.

28. Han J, Hahn MH. Proximal femoral geometry as fracture risk factor in female patients with osteoporotic hip fracture. *J Bone Metab*. 2016;23(3):175-182. https://doi.org/10.11005/jbm.2016.23.3.175

29. El-Kaissi S, Pasco JA, Henry MJ, et al. Femoral neck geometry and hip fracture risk: the Geelong osteoporosis study. *Osteoporos Int*. 2005;16(10):1299-1303. https://doi.org/10.1007/s00198-005-1988-z

30. Tobias JH, Nethander M, Faber BG, et al. Femoral neck width genetic risk score is a novel independent risk factor for hip fractures. *J Bone Miner Res*. 2024;39(3):241-251. https://doi.org/10.1093/jbmr/zjae002

31. Alonso CG, Curiel MD, Carranza FH, Cano RP, Pérez AD. Femoral bone mineral density, neck-shaft angle and mean femoral neck width as predictors of hip fracture in men and women. *Osteoporos Int*. 2000;11(8):714.

32. Deng H-W, Xu F-H, Davies KM, Heaney R, Recker RR. Differences in bone mineral density, bone mineral content, and bone areal size in fracturing and non-fracturing women, and their interrelationships at the spine and hip. *J Bone Miner Metab*. 2002;20(6):358-366. https://doi.org/10.1007/s007740200052

33. Peacock M, Liu G, Carey M, et al. Bone mass and structure at the hip in men and women over the age of 60 years. *Osteoporos Int*. 1998;8(3):231-239. https://doi.org/10.1007/s001980050059

34. Edwards K, Leyland KM, Sanchez-Santos MT, et al. Differences between race and sex in measures of hip morphology: a population-based comparative study. *Osteoarthr Cartil*. 2020;28(2):189-200. https://doi.org/10.1016/j.joca.2019.10.014

35. Siccardi MA, Tariq MA, Valle C. *Anatomy, Bony Pelvis and Lower Limb: Psoas Major*. StatPearls Publishing; 2024.

36. Cruz-Jentoft AJ, Sayer AA. Sarcopenia. *Lancet*. 2019;393(10191):2636-2646. https://doi.org/10.1016/s0140-6736(19)31138-9

37. Rosenberg IH. Sarcopenia: origins and clinical relevance. *Clin Geriatr Med*. 2011;27(3):337-339. https://doi.org/10.1016/j.cger.2011.03.003

38. Hida T, Ishiguro N, Shimokata H, et al. High prevalence of sarcopenia and reduced leg muscle mass in Japanese patients immediately after a hip fracture. *Geriatr Gerontol Int*. 2013;13(2):413-420. https://doi.org/10.1111/j.1447-0594.2012.00918.x

39. Hong W, Cheng Q, Zhu X, et al. Prevalence of sarcopenia and its relationship with sites of fragility fractures in elderly Chinese men and women. *PLoS One*. 2015;10(9):e0138102. https://doi.org/10.1371/journal.pone.0138102

40. Harvey NC, Orwoll E, Kwok T, et al. Sarcopenia definitions as predictors of fracture risk independent of FRAX®, falls, and BMD in the osteoporotic fractures in men (MrOS) study: a meta-analysis. *J Bone Miner Res*. 2021;36(7):1235-1244. https://doi.org/10.1002/jbmr.4293

41. Testa G, Vescio A, Zuccalà D, et al. Diagnosis, treatment and prevention of sarcopenia in hip fractured patients: where we are and where we are going: a systematic review. *J Clin Med*. 2020;9(9):2997. https://doi.org/10.3390/jcm9092997

42. Baird DA, Evans DS, Kamanu FK, et al. Identification of novel loci associated with hip shape: a meta-analysis of genomewide association studies. *J Bone Miner Res*. 2018;34(2):241-251. https://doi.org/10.1002/jbmr.3605

43. Faber BG, Frysz M, Zheng J, et al. The genetic architecture of hip shape and its role in the development of hip osteoarthritis and fracture. *Hum Mol Genet*. 2024;34(3):207-217. https://doi.org/10.1093/hmg/ddae169

44. Zheng J, Frysz M, Faber BG, et al. Comparison between UK Biobank and Shanghai Changfeng suggests distinct hip morphology may contribute to ethnic differences in the prevalence of hip osteoarthritis. *Osteoarthr Cartil*. 2023;33(4):473-481. https://doi.org/10.1016/j.joca.2023.10.006

45. Johnell O, Kanis JA. An estimate of the worldwide prevalence and disability associated with osteoporotic fractures. *Osteoporos Int*. 2006;17(12):1726-1733. https://doi.org/10.1007/s00198-006-0172-4